Gain-of-function *FHF1* mutation causes early-onset epileptic encephalopathy with cerebellar atrophy

Aleksandra Siekierska, PhD*
Mala Isrie, MD*
Yue Liu, MS*
Chloë Scheldeman, MPharm
Niels Vanthillo, MPharm
Lieven Lagae, MD, PhD
Peter A.M. de Witte, MPharm, PhD
Hilde Van Esch, MD, PhD
Mitchell Goldfarb, PhD
Gunnar M. Buyse, MD, PhD

Correspondence to Dr. Buyse: gunnar.buyse@uzleuven.be

ABSTRACT

Objective: Voltage-gated sodium channel (Na_v)–encoding genes are among early-onset epileptic encephalopathies (EOEE) targets, suggesting that other genes encoding Na_v–binding proteins, such as fibroblast growth factor homologous factors (FHFs), may also play roles in these disorders.

Methods: To identify additional genes for EOEE, we performed whole-exome sequencing in a family quintet with 2 siblings with a lethal disease characterized by EOEE and cerebellar atrophy. The pathogenic nature and functional consequences of the identified sequence alteration were determined by electrophysiologic studies in vitro and in vivo.

Results: A de novo heterozygous missense mutation was identified in the *FHF1* gene (*FHF1A*$_{R114H}$, *FHF1B*$_{R52H}$) in the 2 affected siblings. The mutant FHF1 proteins had a strong gain-of-function phenotype in transfected Neuro2A cells, enhancing the depolarizing shifts in $Na_v1.6$ voltage-dependent fast inactivation, predicting increased neuronal excitability. Surprisingly, the gain-of-function effect is predicted to result from weaker interaction of mutant FHF1 with the Na_v cytoplasmic tail. Transgenic overexpression of mutant FHF1B in zebrafish larvae enhanced epileptiform discharges, demonstrating the epileptic potential of this *FHF1* mutation in the affected children.

Conclusions: Our data demonstrate that gain-of-function *FHF* mutations can cause neurologic disorder, and expand the repertoire of genetic causes (*FHF1*) and mechanisms (altered Na_v gating) underlying EOEE and cerebellar atrophy. ***Neurology*® 2016;86:2162–2170**

GLOSSARY

EOEE = early-onset epileptic encephalopathies; **FHF** = fibroblast growth factor homologous factor; **Na_v** = voltage-gated sodium channel; **OE** = overexpression; **WT** = wild-type.

Early-onset epileptic encephalopathies (EOEE) are characterized by progressive diffuse brain dysfunction with recurrent seizures starting during the neonatal or early infantile periods. These epilepsies are among the most severe, with the child typically experiencing multiple seizure types, which are often refractory to antiepileptic drugs, in the setting of developmental delay or regression. Epileptic encephalopathies can worsen over time, and the epileptic activity itself may contribute to severe cognitive, neurologic, and behavioral impairments above and beyond what might be expected from the underlying pathology alone.[1] EOEE represent a broad spectrum of phenotypes that are highly heterogeneous at the clinical and molecular levels. Whereas a number of genetically determined (monogenic) forms have been recognized, in clinical practice many cases remain of unknown etiology.[2] Of the genetic mutations known to be linked to EOEE, several are missense mutations in *SCN8A* encoding the α pore-forming subunits of the voltage-gated sodium channel (Na_v) 1.6,[3–5] with some of these mutations acting in a gain-of-function manner to enhance sodium channel current.[3,4] So far there has been no report of EOEE caused by mutation of sodium channel-binding proteins, such as fibroblast growth factor

Supplemental data at Neurology.org

*These authors contributed equally to this work.

From the Laboratory for Molecular Biodiscovery, Department of Pharmaceutical and Pharmacological Sciences (A.S., C.S., N.V., P.A.M.d.W.), and Laboratory for the Genetics of Cognition (M.I.), University of Leuven; Center for Human Genetics (M.I., H.V.E.) and Child Neurology (L.L., G.M.B.), University Hospitals Leuven; Department of Biological Sciences (Y.L., M.G.), Hunter College of City University, New York; and Graduate Program in Biology/Neuroscience at City University (Y.L.), New York, NY.

Go to Neurology.org for full disclosures. Funding information and disclosures deemed relevant by the authors, if any, are provided at the end of the article.

homologous factors (FHFs), although *FHF* loss-of-function mutations have been associated with unrelated neurologic disorders (spinocerebellar ataxia and Wildervanck syndrome). We have identified a new EOEE gene (*FHF1*) by whole-exome sequencing in a family quintet with 2 affected siblings, and we validated the disease-causative nature and mechanism by functional electrophysiologic studies in vitro and in vivo.

METHODS

Genetic analysis of the EOEE-affected family. Pathogenic copy number variants were excluded by conventional karyotyping and array comparative genomic hybridization. DNA of parents, their 2 affected children, and 1 unaffected child was extracted from peripheral blood lymphocytes. All 5 samples were used for library preparation and exome enrichment using the TruSeq DNA library prep kit (Illumina, San Diego, CA) and NimbleGen SeqCap EZ Human Exome Library v3, respectively. Paired-end sequencing (2 × 100 bp) was performed on the HiSeq 2000 platform (Illumina). Sequence reads were mapped to the human reference genome (hg19) with BWA and variant calling was performed using the GATK framework.[6,7] Variants were annotated in Annovar and filtered in Microsoft (Redmond, WA) Excel based on inheritance pattern, location, function, and presence in the 1000 Genomes dataset.[8] Candidate variants obtained from exome sequencing were validated using Sanger sequencing. Primers covering all exons and exon–intron boundaries were designed using Primer3Plus.[9] PCR was performed using GoTaq DNA polymerase (Promega Corporation, Madison, WI) and products were sequenced on an ABI3130xl sequencer (Life Technologies, Carlsbad, CA).

Electrophysiologic recordings of $Na_v1.6$-derived sodium current in the presence of wild-type and mutant FHF1 proteins. Expression of tetrodotoxin-resistant murine $Na_V1.6^{TTXr}$ ($Na_V1.6_{Y371S}$) cDNA in pIRESneo3 (Clontech, Mountain View, CA) and bicistronic expression of FHF and green fluorescent protein in pIRES2-ZsGreen1 (Clontech) were described previously.[10] Missense mutations (*FHF1A*$_{R114H}$, *FHF1B*$_{R52H}$, *FHF1B*$_{R52A}$, *FHF1B*$_{R52G}$) were generated using complementary mutagenic primers. Neuro2A cells were transfected with FHF and $Na_V1.6^{TTXr}$ expressing plasmids at 2:1 ratio using Lipofectamine 2000, transferred to glass coverslips after 2 hours, and used for recordings after 24–48 hours. Coverslips were placed in the recording chamber of a Nikon (Tokyo, Japan) EF600 microscope filled with O_2:CO_2 (95:5)–bubbled extracellular solution (in mM): 109 NaCl, 26 $NaHCO_3$, 10 HEPES, 4.7 KCl, 11 glucose, 1.2 $MgCl_2$, 2 $CaCl_2$, 0.2 $CdCl_2$, 3 myo-inositol, 2 Na pyruvate, 0.001 TTX (buffered to pH 7.2 with NaOH), and green fluorescent cells were whole-cell patched using micropipettes (1–2 MΩ resistance) filled with 104 CsF, 50 tetraethylamine Cl, 10 HEPES, 5 glucose, 2 $MgCl_2$, 10 EGTA, 2 Na_2ATP, and 0.2 Mg GTP (buffered to pH 7.2 with CsOH). Voltage clamp was conducted using an Axopatch 200B amplifier, Digidata 1322 digital/analog interface, and pCLAMP9 software (Molecular Devices, Sunnyvale, CA). Recording signals were filtered at 5 kHz and digitized at 10 or 20 kHz. To measure evoked sodium currents, capacitive and leak currents were subtracted during data acquisition using the presweep hyperpolarizing P/N method in the pCLAMP9 software. Protocols for measuring voltage dependence of sodium channel activation and steady-state inactivation were described previously.[10] The statistical significance between 2 conditions was calculated by the 2-tailed Student *t* test. For each cell analyzed for voltage dependence of activation and steady-state (fast) inactivation, data at all tested voltages were fit to a Boltzmann equation to establish $V_{1/2}$ and slope *k* values using Clampfit10, and the values for all cells recorded under the same conditions were expressed and graphed as mean ± SEM.

Zebrafish overexpression studies. ***Zebrafish maintenance and breeding.*** Adult zebrafish (*Danio rerio*) of the AB strain (ZIRC) were maintained at 28.5°C on a 14-hour light/10-hour dark cycle under standard aquaculture conditions. Embryos were raised in embryo medium, containing (in mM) 1.5 HEPES, pH 7.6, 17.4 NaCl, 0.21 KCl, 0.12 $MgSO_4$, and 0.18 Ca $(NO_3)_2$, in an incubator on a 14-hour light/10-hour dark cycle at 28.5°C.

Overexpression experiments. Wild-type (WT) zebrafish *fhf1b1* cDNA (ENSDART00000090596) under the control of the zebrafish CNS-specific her4 promoter was cloned into the Tol2 expression vector (gift from G. Weidinger, University of Ulm, Germany) using *Pac*I and *Not*I sites (WT-*fhf1b1*-Tol2). The mutation encoding R56H in zebrafish was cloned into the *fhf1b1* sequence via site-directed mutagenesis (primers: table e-1 on the *Neurology*® Web site at Neurology.org) (R56H-*fhf1b1*-Tol2). Empty Tol2 vector expressing the fluorescent reporter mCherry alone was used as a control (ctrl-Tol2). The overexpression experiment was performed by cytoplasmic microinjection of 10 pg of WT-*fhf1b1*-Tol2, R56H-*fhf1b1*-Tol2, or ctrl-Tol2 and 50 pg of transposase (1-nL volume) into embryos at the one-cell stage.

fhf1b1 mRNA expression analysis. Total RNA from 5 dpf larvae was extracted using TRIzol (Ambion; Thermo Fisher Scientific, Waltham, MA). Reverse transcription of total RNA to single-stranded cDNA was performed using the High-Capacity cDNA Reverse Transcription Kit (Applied Biosystems, Foster City, CA). Measurements of *fhf1b1* mRNA were performed using *fhf1b1*-specific primers (primers: table e-1) combined with SsoAdvanced Universal SYBR Green Supermix (Bio-Rad, Hercules, CA) using CFX96 Touch Real-Time PCR Detection System (Bio-Rad) and analyzed using CFX Manager Software (Bio-Rad). *fhf1b1* transcripts were normalized against β-2 microglobulin and β-actin controls (table e-1). The results consist of data from 3 separate experiments run in triplicate. Pairwise statistical significance was determined with Student unpaired *t* test (Prism 6; GraphPad, La Jolla, CA).

Tectal field recordings. Open-field recordings were obtained from zebrafish larval tecta at 5 dpf at room temperature, as described previously.[11] Single recordings were performed for 10 minutes. Spontaneous events were taken into account when the amplitude exceeded baseline by at least threefold. The analysis of spikes was carried out using Clampfit 10.2 software (Molecular Devices). The statistical significance between 2 conditions was calculated by Fisher exact test (GraphPad Prism 6).

Standard protocol approvals, registrations, and patient consents. This study was approved by the UZ Leuven institutional review board and written patient informed consent was obtained. All zebrafish experiments were approved by the KU Leuven Ethics Committee and the Belgian Federal authority.

RESULTS

***FHF1* mutation identified in EOEE with cerebellar atrophy.** We carried out whole-exome sequencing on a family quintet with 2 affected siblings (EOEE with cerebellar atrophy) and

unaffected parents and sibling, where extensive neurometabolic investigations and directed mutagenesis analysis of known genes (including *STXBP1*, *KCNQ2*, *SLC2A1*) were all negative. Exome data analysis identified a heterozygous missense mutation in *FHF1* on chromosome 3 (NM_021032, 192053223C>T based on Hg19, p.R114H in A-isoform, p.R52H in B-isoform; figure 1A). This was the only variant present in the 2 affected siblings but not in the unaffected sibling, their parents (pointing towards germline mosaicism), or in normal population databases including 1000 Genomes, the NHLBI Exome Variant Server, and the EXaC browser. No other pathogenic mutations were yielded by filtering variants for recessive (homozygous or compound heterozygous) inheritance present in both affected individuals and absent in the unaffected sibling. The affected arginine residue is part of the highly conserved surface region that binds voltage-gated sodium channels (figure 1, B–D),[12,13] and the mutation was presumed to be damaging by

Figure 1 **Heterozygous missense mutation (C>T) in *FHF1* in 2 siblings with early-onset epileptic encephalopathy (EOEE) with cerebellar atrophy**

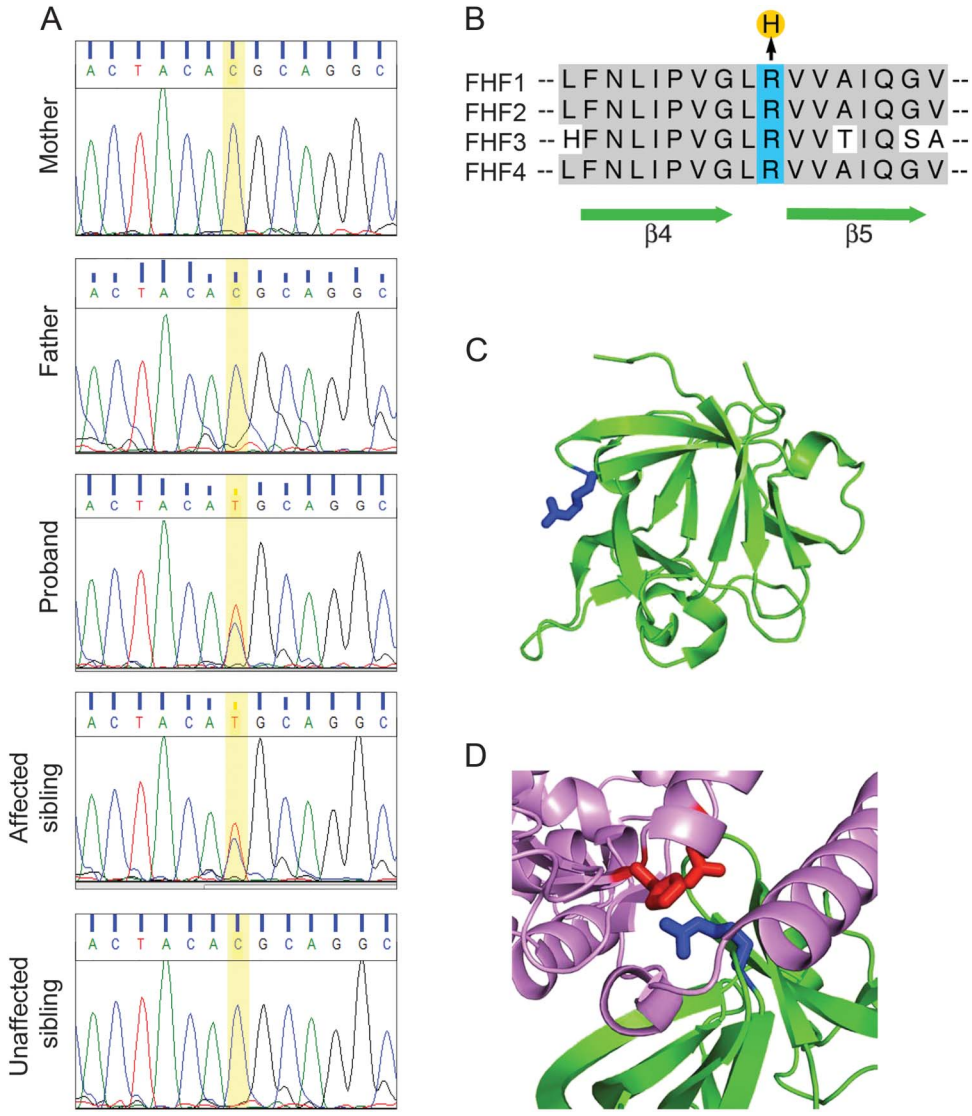

(A) Whole-exome sequencing on a family quintet with 2 affected siblings (EOEE with cerebellar atrophy) and unaffected parents and sibling identified a heterozygous missense mutation in *FHF1* (p.R114H in A-isoform, p.R52H in B-isoform). (B) Alignment of fibroblast growth factor homologous factor (FHF) sequences in the region of mutation. The FHF1 amino acid sequence contributing to the β4 and β5 strands and the β4/β5 loop is highly conserved among the 4 FHF core domains (shaded residues), including the β4/β5 loop arginine (blue) that is mutated to histidine (orange) in the affected siblings. (C) Ribbon diagram of the FHF1 core structure.[22] The affected arginine residue side chain (blue) in the β4/β5 loop projects to the protein surface. (D) Ribbon diagram of the FHF/voltage-gated sodium channel (Nav) interface.[13] The FHF β4/β5 loop arginine (blue) interacts with aspartate and histidine residues (red) in the Nav cytoplasmic tail.

PolyPhen-2 and Mutationtaster in silico prediction software (Grantham score 29; GERP score 5.16).[14,15] A disease-causative nature of the mutation was further supported by the physiologic role of FHF1 in controlling neuronal excitability,[16–18] the patients' phenotype being dominated by a hyperexcitable CNS state with epilepsy/EOEE and cerebellar atrophy assumed secondary to chronic excitotoxicity.

Clinical phenotype. The proband (female) was born at term (birthweight 2,920 g) as the first child of nonconsanguineous Caucasian parents. It was a spontaneous twin pregnancy with in utero loss of the other fetus around the end of the first trimester (no medical information available). Tonic seizures developed from the age of 14 days, mostly during sleep. She was a normal neonate prior to the onset of the seizures. There was no epileptic myoclonus or other seizure types. Very rapidly, a clear encephalopathic EEG developed with severe background slowing and multifocal epileptic abnormalities. Seizures were tonic, generalized or focal with a typical ictal EEG pattern of low voltage fast activity (figure e-1), followed by long suppression of the background. This evolution resulted in a hypsarrhythmia pattern at the age of 5 months, without clinical epileptic spasms. Her epilepsy proved refractory to multiple antiepileptic drugs. She developed profound intellectual disability, acquired microcephaly, axial hypotonia, ataxia (limbs), severe feeding difficulties necessitating tube feeding, cerebral visual impairment, and absent speech development. Unsupported sitting was achieved at age 24 months; she never came to standing and walking. Visual evoked potentials were normal at age 4 months; funduscopy was normal initially and showed pale optic discs and narrow vessels at age 5 years. Brain MRI was normal at age 5 months, but showed cerebellar atrophy at age 6 years (figure 2A). The disease course seemed degenerative (decrease in alertness, general condition, and skills; appearance of discomfort and agitation; increase in epilepsy) prior to death at age 7 years due to status epilepticus. The proband had 2 younger brothers. The youngest was healthy; the other showed an identical clinical course as his sister with refractory epilepsy (onset at age 4 weeks, tonic seizures) with similar seizure semiology and EEG abnormalities, hypotonia, ataxia, acquired microcephaly, poor visual contact, feeding problems, and profound intellectual disability. Brain MRI was normal at age 2 months but showed cerebellar atrophy at age 3 years (figure 2B). He died at age 3.5 years (cause of death unknown). At the age of 5 years, the father had one epileptic seizure (unknown whether febrile or not); further family history was negative for epilepsy and neurodegenerative disease.

***FHF1* R→H mutation and sodium channel inactivation.** FHFs are small cytosolic proteins that interact with the cytoplasmic tails of Na_v and promote excitability by elevating the voltage dependence of neuronal sodium channel fast inactivation.[10,16,19–21] In order to determine the functional consequence of the EOEE-associated FHF1 R→H substitution within the core domain, WT or mutant A- or B-isoforms of FHF1 ($FHF1A_{R114H}$ and $FHF1B_{R52H}$) were expressed in Neuro2A cells by transient DNA transfection together with sodium channel $Na_v1.6$, and channel inactivation gating was measured by whole-cell voltage clamp protocols. WT FHF1B ($FHF1B_{WT}$) induced a small depolarizing shift in the voltage dependence of $Na_v1.6$ inactivation, from $V_{1/2} = -81.4 \pm 1.6$ mV (n = 7) without FHF to $V_{1/2} = -74.9 \pm 1.3$ mV (n = 8) with $FHF1B_{WT}$ (figure 3, A and B). In comparison,

Figure 2 Cerebellar atrophy in 2 siblings with a gain-of-function *FHF1* mutation

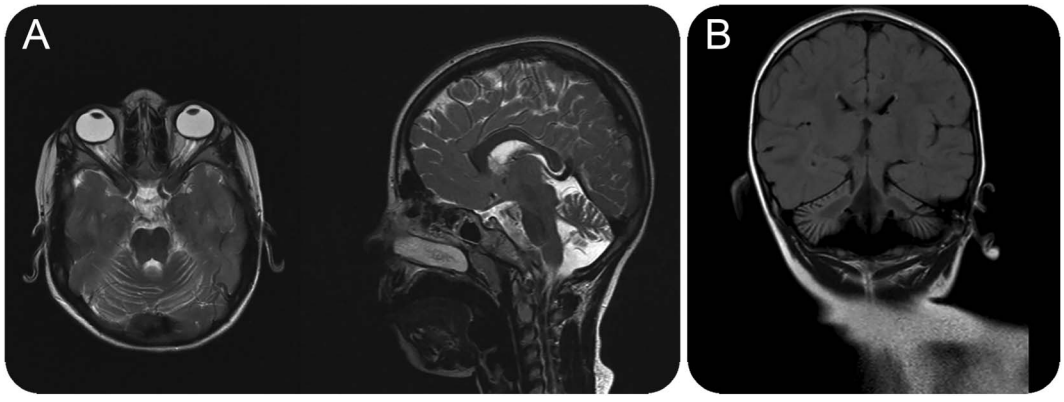

MRI of the brain was normal at infant age in both affected siblings. However, repeat MRI in their further disease course, which was degenerative, showed the emergence of cerebellar atrophy in both children: (A) proband at age 6 years: axial and sagittal image show prominent fissures between shrunken cerebellar folia; (B) younger brother of proband at age 3 years: coronal image shows cerebellar atrophy.

Figure 3 Substitutions at FHF1B-R52/FHF1A-R114 are gain-of-function for inactivation gating of voltage-gated sodium channel (Na_v) 1.6

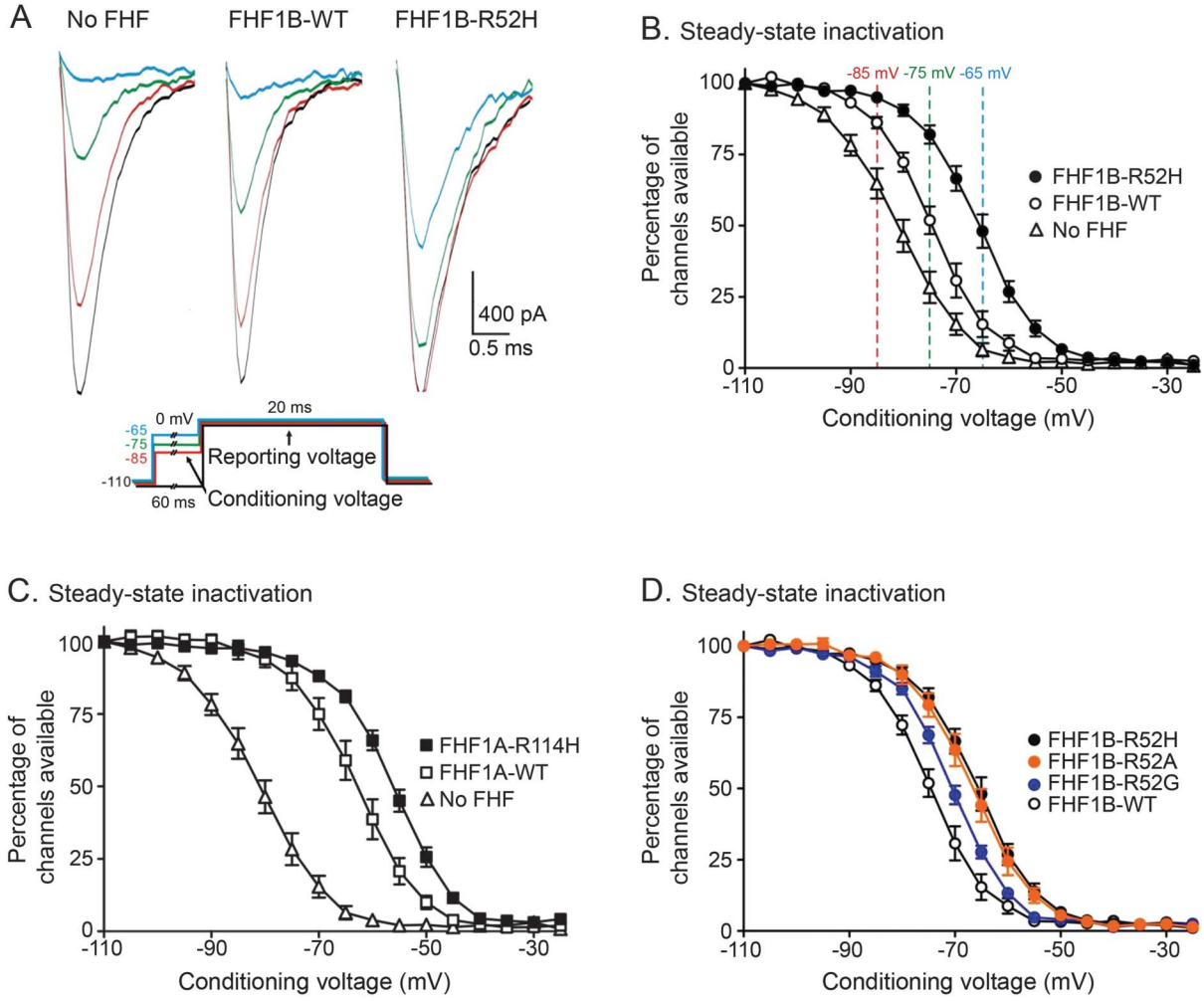

(A, B) Voltage dependence of $Na_v1.6$ steady-state inactivation in the presence of $FHF1B_{WT}$, $FHF1B_{R52H}$, or no fibroblast growth factor homologous factor (FHF). Sodium currents from noninactivated channels were measured at the reporting voltage (0 mV) following 60 ms conditioning voltages ranging from −110 to −25 mV. Superimposed sodium currents (A, above) recorded during the reporting voltage from several conditioning voltages (A, below) show that there is larger percentage of maximal sodium current after a given conditioning voltage in presence of FHF1B compared to no FHF, and the percentage of maximal current is larger still in the presence of $FHF1B_{R52H}$. $Na_v1.6$ inactivation in cells without FHF (n = 7, $V_{1/2}$ −81.4 ± 1.6 mV), with $FHF1B_{WT}$ (n = 8, $V_{1/2}$ −74.9 ± 1.3 mV), and with $FHF1B_{R52H}$ (n = 9, $V_{1/2}$ −65.8 ± 1.3 mV, $p < 0.0002$ vs $FHF1B_{WT}$) (B). Dotted lines indicate the color-coded conditioning voltages in A. (C) Voltage dependence of steady-state $Na_v1.6$ inactivation in cells without FHF (n = 7, $V_{1/2}$ −81.4 ± 1.6 mV), with $FHF1A_{WT}$ (n = 7, $V_{1/2}$ −63.4 ± 1.6 mV), and with $FHF1A_{R114H}$ (n = 8, $V_{1/2}$ −56.4 ± 0.9 mV, $p < 0.004$ vs $FHF1A_{WT}$). (D) $Na_v1.6$ inactivation in presence of $FHF1B_{WT}$ (n = 8, $V_{1/2}$ −74.9 ± 1.3 mV), $FHF1B_{R52H}$ (n = 9, $V_{1/2}$ −65.8 ± 1.3 mV), $FHF1B_{R52G}$ (n = 9, $V_{1/2}$ −70.7 ± 0.7 mV, $p < 0.02$ vs $FHF1B_{WT}$), or $FHF1B_{R52A}$ (n = 8, $V_{1/2}$ −67.1 ± 1.5 mV, $p < 0.002$ vs $FHF1B_{WT}$). All substitutions at FHF1B-Arg52 are gain-of-function. (B–D) Percentage of channels available after each conditioning voltage expressed and graphed as mean ± SEM.

$FHF1B_{R52H}$ had a significantly stronger effect on $Na_v1.6$, elevating $V_{1/2}$ to −65.8 ± 1.3 mV (n = 9, $p < 0.0002$, $FHF1B_{R52H}$ vs $FHF1B_{WT}$) (figure 3, A and B). The R→H substitution in the FHF1A isoform also increased modulation of channel inactivation compared to $FHF1A_{WT}$. $FHF1A_{WT}$ exerted a strong effect on inactivation, with $V_{1/2}$ = −63.4 ± 1.6 mV (n = 7) (figure 3C), as previously reported.[10] Nonetheless, $FHF1A_{R114H}$ induced even stronger channel modulation, with $V_{1/2}$ = −56.4 ± 0.9 mV (n = 8, $p < 0.004$) (figure 3C). Thus, the EOEE-associated *FHF1* missense mutation acts in a gain-of-function manner on sodium channel gating, predicting increased neuronal excitability. While FHF expression altered inactivation gating, there were no significant effects on channel activation (data not shown).

The FHF1 arginine residue affected by the EOEE-associated missense mutation is conserved among all FHF family proteins and is part of the binding interface with the sodium channel tail that is necessary for FHF modulation of Na_v fast inactivation gating.[12,13,22] In order to test whether the gain-of-function FHF1 R→H substitution results from

Figure 4 R56H *fhf1b1* overexpression (OE) causes epileptiform discharges in transgenic zebrafish larvae

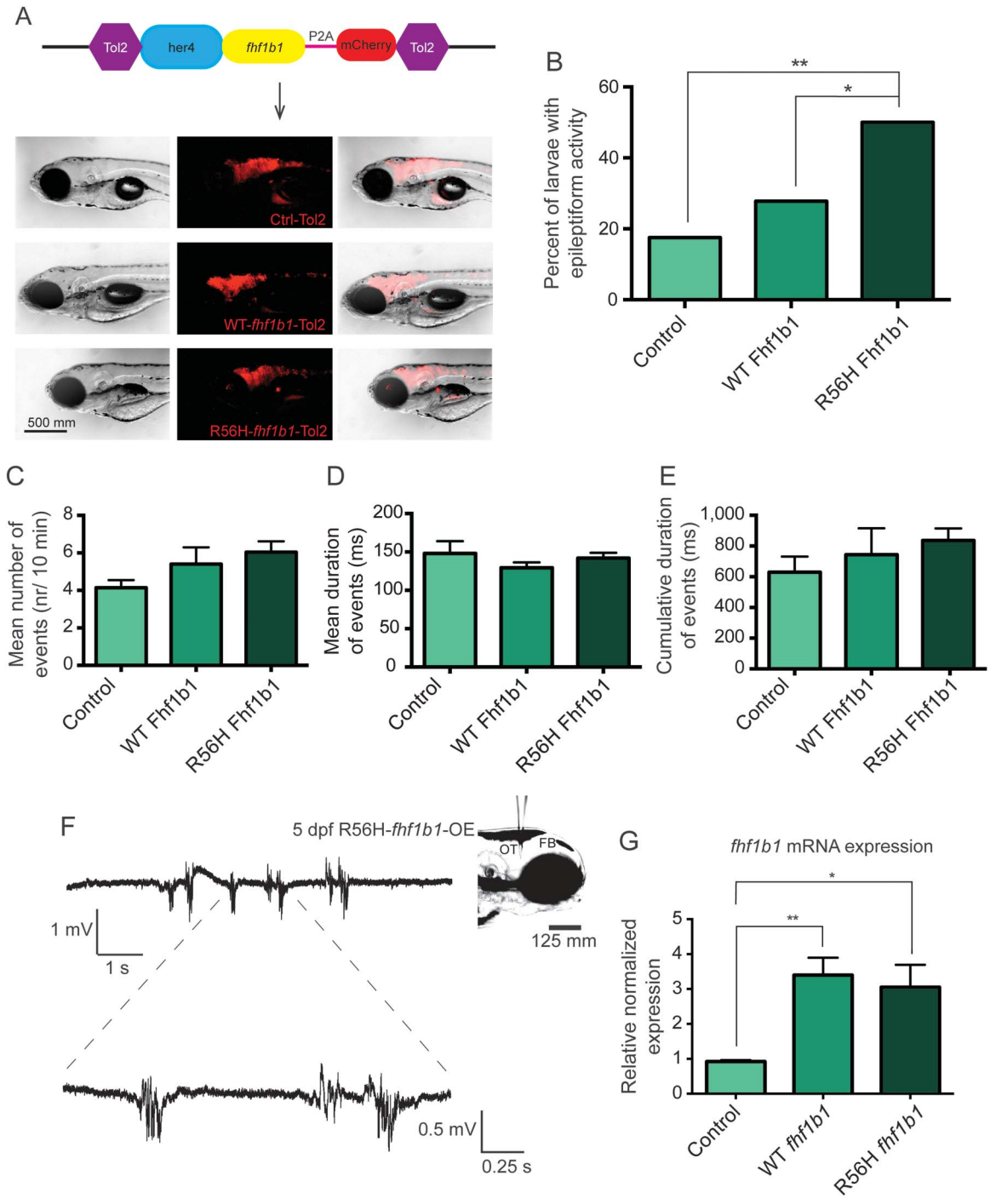

(A) The Tol2 system was used to transiently overexpress wild-type (WT) and R56H mutant zebrafish *fhf1b1*. WT and R56H zebrafish *fhf1b1* cDNA was expressed under the control of the zebrafish CNS-specific her4 promoter. A fluorescent reporter mCherry was used to identify larvae with *fhf1b1* expression. Self-cleaving peptide, P2A, enabled the separation between fhf1b1 and mCherry in order to avoid possible disadvantages of a fusion protein. Representative images of 5 dpf larvae microinjected with zebrafish cDNA encoding WT and mutated *fhf1b1*, selected for tectal field recordings and mRNA analysis. Red fluorescence depicts the brain-specific expression of Fhf1b. Scale bar, 500 μm. (B) Percentage of larvae with abnormal epileptiform activity after overexpression of WT and R56H *fhf1b1*. Overexpression of mutant Fhf1b led to a significant increase of the number of larvae with seizure-like events in comparison to WT-*fhf1b1*-OE and control larvae (27/54 larvae with R56H-*fhf1b1*-OE vs 15/54 larvae with WT-*fhf1b1*-OE and 7/40 control larvae; **p* = 0.0293 and ***p* = 0.0012, respectively, Fisher exact test). Overexpression of mCherry alone resulted in 17.5% of seizing larvae, which was not statistically different from 27.8% for WT-*fhf1b1*-OE larvae (*p* = 0.3261, Fisher exact test). (C) Occurrence of epileptiform events/recording in WT-*fhf1b1*-OE (5.4 ± 0.9), R56H-*fhf1b1*-OE (6.0 ± 0.6), and control larvae (4.1 ± 0.4) (*p* = 0.3237, one-way analysis of variance [ANOVA]). Results are mean ± SEM. (D) Mean duration of epileptiform events in WT-*fhf1b1*-OE (129.4 ± 7.1 ms), R56H-*fhf1b1*-OE (141.9 ± 7.0 ms), and control larvae (148.2 ± 16.0 ms) (*p* = 0.4112, one-way ANOVA). Results are mean ± SEM. (E) Cumulative duration of epileptiform events in WT-*fhf1b1*-OE (743.6 ± 172.1 ms), R56H-*fhf1b1*-OE (836.5 ± 78.3 ms), and control larvae (629.3 ± 102.1 ms) (*p* = 0.5556, one-way ANOVA). Results are mean ± SEM. (F) Representative spontaneous

Continued

a property of the substituted histidine side chain as opposed to the loss of the wild-type arginine residue, R→A and R→G substitutions in FHF1B were tested for their effects on channel inactivation. As shown in figure 3D, $FHF1B_{R52A}$ was nearly as potent as $FHF1B_{R52H}$ at elevating $Na_v1.6$ steady-state inactivation ($V_{1/2} = -67.1 \pm 1.5$ mV, n = 8, $p < 0.002$, $FHF1B_{R52A}$ vs $FHF1B_{WT}$), while $FHF1B_{R52G}$ also exerted a significant, but weaker, gain-of-function effect ($V_{1/2} = -70.7 \pm 0.7$ mV, n = 9, $p < 0.02$, $FHF1B_{R52G}$ vs $FHF1B_{WT}$). These findings were surprising, as $FHF1B_{R52G}$ had previously been shown to bind to purified $Na_v1.6$ tail fragment in vitro with 19-fold lower affinity than did $FHF1B_{WT}$.[12] Thus, while FHF binding to sodium channel tail is essential for modulation of channel inactivation gating, the specific FHF arginine side-chain interactions with channel may serve to limit FHF physiologic function.

WT vs mutated Fhf1b in zebrafish. To further investigate the pathogenic nature and functional consequences of the patients' *FHF1* R→H mutation, we established an Fhf1 overexpression model in zebrafish larvae. Zebrafish have 2 *fhf1* genes (due to genome duplication), termed *fhf1a* and *fhf1b*. The A-type protein isoforms (Fhf1a, Fhf1b2) encoded by these 2 zebrafish genes share 81.8%–90.9% identity with human FHF1A, whereas the B-type protein isoform Fhf1b1 encoded by an alternatively spliced mRNA from the zebrafish *fhf1b* is 84.4% identical to human FHF1B. The zebrafish *fhf1b* gene expresses both A- (Fhf1b2) and B-type (Fhf1b1) zebrafish isoforms (figure e-2). The arginine residue mutated in the EOEE siblings is conserved in zebrafish *fhf1* orthologs and corresponds to R112 in A-isoform Fhf1a, R116 in A-isoform Fhf1b2, and R56 in B-isoform Fhf1b1 (figure e-2). In contrast to B-type FHF isoforms that are only proexcitatory, A-type FHF isoforms also have inhibitory effects on neural excitation due to the long-term sodium channel blocking particle residing at the N-termini of these proteins.[10,18] Therefore, the zebrafish *fhf1b1* transcript encoding the B-type isoform (Fhf1b1) was selected for in vivo transgenesis experiments.

To introduce WT and mutant *fhf1b1* into zebrafish genome, Tol2 tissue-specific transgenesis was used.[23] Zebrafish *fhf1b1* was cloned under the CNS-specific promoter her4 and mCherry was used to identify the embryos with Fhf1b1 expression (figure 4A). One-cell stage zebrafish embryos were microinjected with WT and R56H-*fhf1b1*-Tol2 overexpression constructs. *fhf1b1*-Tol2-injected larvae did not exhibit any gross dysmorphologies compared to control larvae (i.e., injected with empty Tol2 vector and expressing mCherry only) (figure 4A). For further experiments, normal-looking embryos displaying touch response were selected. To investigate whether overexpression (OE) of R56H *fhf1b1* resulted in abnormal brain activity, we performed local field potential recordings[11] on larval optic tecta at 5 days postfertilization WT-*fhf1b1*-OE (n = 54), R56H-*fhf1b1*-OE (n = 54), and controls (n = 40). Recurrent epileptiform discharges occurred in 50% of R56H-*fhf1b1*-OE larvae, which was of significantly greater incidence than in WT-*fhf1b1*-OE and control groups (27.8% and 17.5%, respectively) (figure 4B). The mean frequency, duration, and cumulative duration of events did not significantly differ among tested groups (figure 4, C–E). Abnormal epileptiform activities observed in R56H-*fhf1b1*-OE larvae consisted of bursts with amplitude exceeding the baseline by at least 3-fold (representative example in figure 4F). Real-time qPCR experiments confirmed that both WT and R56H *fhf1b1* were effectively and equally overexpressed in the OE larvae (figure 4G), confirming that the difference between the number of seizing fish was a result of the *fhf1b1* alteration and not due to the differences in the mRNA expression. These results demonstrate the epileptic potential of the *fhf1b1* mutation in an in vivo zebrafish model, supporting FHF1 gain-of-function as the disease mechanism in our EOEE patients with *FHF1* missense mutation.

DISCUSSION Our data demonstrate that gain-of-function *FHF1* mutation causes human disease (familial EOEE with progressive cerebellar atrophy). Together with other recent studies,[3–5] our findings suggest an FHF/Na_v axis underlying EOEE. This is the first disorder linked with *FHF1* and with *FHF* gene gain-of-function. Our findings also reveal an unexpected relationship between FHF/Na_v interaction and neuronal sodium channel fast inactivation gating.

The de novo heterozygous missense *FHF1* mutation identified in 2 siblings with a lethal disorder characterized by EOEE and cerebellar atrophy was the only variant present in the affected siblings but

Figure 4 legend, continued:
epileptiform activity recorded from 5 dpf R56H-*fhf1b1*-OE larvae. Top trace represents typical epileptiform pattern as seen in gap-free recordings. Bottom trace shows high-resolution magnification of the selected epileptiform events. Next to the traces, an agar immobilized 5 dpf zebrafish with the recording electrode placed in the optic tectum (OT) is shown. FB = forebrain. (G) *fhf1b1* mRNA expression in WT and R56H-*fhf1b1*-OE larvae. *fhf1b1* was expressed approximately 3-fold higher in WT and mutant-OE larvae in comparison to *fhf1b1* baseline level in control larvae. **$p = 0.0080$ WT-*fhf1b1*-OE vs control; *$p = 0.0293$ R56H-*fhf1b1*-OE vs control (2-tailed Student *t*-test). β-2 microglobulin and β-actin were used as normalizing controls. Values are mean ± SEM (triplicate samples with triplicate qPCR experiments).

not in the unaffected family members or in normal population databases, and no other pathogenic variants were identified. In transfected Neuro2A cells, the EOEE-associated FHF1 R→H substitution in either FHF1A or FHF1B isoforms right-shifted voltage dependence of Na_v fast inactivation due to arginine side chain loss within the FHF/Na_v interface, predicting increased neuronal excitability. Transgenic overexpression of zebrafish $Fhf1b1_{R56H}$ replicated epileptiform discharges in larval-stage animals. Interestingly, our findings highlight the requirement for titrated *FHF* gene function in maintaining normal human brain activity and prevention of epilepsy. Thus, while *FHF4* loss-of-function induces spinocerebellar ataxia and *FHF2* loss-of-function can cause Wildervanck syndrome,[24,25] the *FHF1* missense mutation described here induces epileptic encephalopathy through a gain-of-function mechanism. These findings contrast with *FHF2* gene loss-of-function, which has been shown to induce epilepsy (generalized epilepsy with febrile seizures plus).[26]

All FHFs are small cytosolic proteins that interact with the cytoplasmic tails of Na_v and elevate the voltage dependence of neuronal sodium channel fast inactivation.[10,16,19–21] Each *FHF* gene can encode multiple protein isoforms differing in their N-terminal domains fused to the channel-binding β-trefoil core common to all isoforms.[27] The EOEE-inducing *FHF1* missense mutation replaces an arginine residue in the β4-β5 loop (figure 1, B and C) that contributes to the highly conserved structural interface between FHF proteins and sodium channel cytoplasmic tails (figure 1D). While the FHF/Na_v interface is essential for FHF modulation of Na_v inactivation and the FHF β4-β5 loop arginine residue makes a strong contribution to FHF/Na_v interaction,[12,13] our data show that replacement of this arginine with any of 3 unrelated residues paradoxically enhances modulation of Na_v inactivation gating. Thus, while FHF binding to the sodium channel tail is essential for modulation of channel inactivation gating, the specific FHF arginine side-chain interactions with the channel may serve to limit FHF physiologic function. Consistent with our findings, a highly conserved aspartate residue (D1866) in the sodium channel tail of $Na_v1.1$ that contacts the arginine side chain in the FHF β_4-β_5 loop (figure 1D) is itself a site of missense mutation associated with genetic epilepsy with febrile seizures plus.[28] Similar to the *FHF1* mutation described in this report, the $Na_v1.1_{D1866Y}$ epilepsy-associated substitution has also been reported to raise the voltage dependence of channel inactivation.[28] In addition, a cardiac $Na_v1.5_{H1849R}$ substitution at another residue contacting the FHF β_4-β_5 loop also raises the voltage dependence of inactivation for this sodium channel and causes a cardioarrhythmia associated with prolonged myocyte sodium current.[29] Understanding the mechanisms by which mutations in sodium channels or their associated proteins impact fast inactivation gating and human disease still awaits the elucidation of vertebrate sodium channel structures in the closed, open, and inactivated states.

Cerebellar atrophy, a component of the disease phenotype associated with mutated *FHF1* (this report), has previously been reported in EOEE caused by mutations in several other genes including those encoding voltage-gated sodium channels such as *SCN8A*.[5,30,31] Currently, it is not clear how mutations in these genes cause brain atrophy, but one possible mechanism is through a hyperexcitotoxic mechanism. The cerebellar-specific atrophy associated with *FHF1* mutation mirrors the preferential cerebellar functional deficit associated with *FHF1* gene deletion[16] and could reflect preferential expression of an FHF1 protein isoform compared to other FHFs in this brain region.

Our findings offer a causal link between familial EOEE with cerebellar atrophy and *FHF1* mutation and report the demonstration of a gain-of-function *FHF* missense mutation at the FHF/Na_v interface. EOEEs are severe neurologic disorders, which in clinical practice often remain of undetermined etiology. In recent years, progress in molecular diagnostics has revealed that a significant proportion of EOEE are single-gene disorders. Identification of a causative gene defect is important for prognostic and genetic counseling, and may also carry treatment implications. The current study adds *FHF1* and altered Na_v gating to the list of EOEE genes and mechanisms, and our findings support the inclusion of *FHF* genes into the panels of candidate genes used to query the genetic basis of EOEE in additional affected individuals.

AUTHOR CONTRIBUTIONS

All authors participated in the design of experiments and experimental work, data analyses and interpretations, and in the writing and critical revision of the manuscript, which has been approved by each author.

ACKNOWLEDGMENT

G.M. Buyse and H. Van Esch are Senior Clinical Investigators of the Research Foundation–Flanders (FWO Vlaanderen, Belgium). The authors thank Patrik Verstreken (VIB, KU Leuven) for providing access to the electrophysiology equipment and Jan Maes (LMB, KU Leuven) for help with zebrafish cytoplasmic microinjections.

STUDY FUNDING

Supported by Public Health Services grant R01-GM098540 awarded to M. Goldfarb and Geconcerteerde Onderzoeks Actie (GOA 2011–2015) and IUAP (BELSPO-IAP program through the project IAP P7/43-BeMGI) (HVE). G.M. Buyse and H. Van Esch are Senior Clinical Investigators of the Research Foundation–Flanders (FWO Vlaanderen, Belgium).

DISCLOSURE

The authors report no disclosures relevant to the manuscript. Go to Neurology.org for full disclosures.

Received January 6, 2016. Accepted in final form March 12, 2016.

REFERENCES

1. Berg AT, Berkovic SF, Brodie MJ, et al. Revised terminology and concepts for organization of seizures and epilepsies: report of the ILAE Commission on Classification and Terminology, 2005–2009. Epilepsia 2010;51:676–685.
2. Tavyev Asher YJ, Scaglia F. Molecular bases and clinical spectrum of early infantile epileptic encephalopathies. Eur J Med Genet 2012;55:299–306.
3. Veeramah KR, O'Brien JE, Meisler MH, et al. De novo pathogenic SCN8A mutation identified by whole-genome sequencing of a family quartet affected by infantile epileptic encephalopathy and SUDEP. Am J Hum Genet 2012;90:502–510.
4. Estacion M, O'Brien JE, Conravey A, et al. A novel de novo mutation in SCN8A (Nav1.6) with enhanced channel activation in a child with epileptic encephalopathy. Neurobiol Dis 2014;69:117–123.
5. Ohba C, Kato M, Takahashi S, et al. Early onset epileptic encephalopathy caused by de novo SCN8A mutations. Epilepsia 2014;55:994–1000.
6. Li H, Durbin R. Fast and accurate short read alignment with Burrows-Wheeler transform. Bioinformatics 2009;25:1754–1760.
7. McKenna A, Hanna M, Banks E, et al. The Genome Analysis Toolkit: a MapReduce framework for analyzing next-generation DNA sequencing data. Genome Res 2010;20:1297–1303.
8. Wang K, Li M, Hakonarson H. ANNOVAR: functional annotation of genetic variants from high-throughput sequencing data. Nucleic Acids Res 2010;38:e164.
9. Rozen S, Skaletsky H. Primer3 on the WWW for general users and for biologist programmers. Methods Mol Biol 2000;132:365–386.
10. Dover K, Solinas S, D'Angelo E, Goldfarb M. Long-term inactivation particle for voltage-gated sodium channels. J Physiol 2010;588:3695–3711.
11. Schubert J, Siekierska A, Langlois M, et al. Mutations in STX1B, encoding a presynaptic protein, cause fever-associated epilepsy syndromes. Nat Genet 2014;46:1327–1332.
12. Goetz R, Dover K, Laezza F, et al. Crystal structure of a fibroblast growth factor homologous factor (FHF) defines a conserved surface on FHFs for binding and modulation of voltage-gated sodium channels. J Biol Chem 2009;284:17883–17896.
13. Wang C, Chung BC, Yan H, Lee SY, Pitt GS. Crystal structure of the ternary complex of a NaV C-terminal domain, a fibroblast growth factor homologous factor, and calmodulin. Structure 2012;20:1167–1176.
14. Adzhubei IA, Schmidt S, Peshkin L, et al. A method and server for predicting damaging missense mutations. Nat Methods 2010;7:248–249.
15. Schwarz JM, Cooper DN, Schuelke M, Seelow D. MutationTaster2: mutation prediction for the deep-sequencing age. Nat Methods 2014;11:361–362.
16. Goldfarb M, Schoorlemmer J, Williams A, et al. Fibroblast growth factor homologous factors control neuronal excitability through modulation of voltage-gated sodium channels. Neuron 2007;55:449–463.
17. Shakkottai VG, Xiao M, Xu L, et al. FGF14 regulates the intrinsic excitability of cerebellar Purkinje neurons. Neurobiol Dis 2009;33:81–88.
18. Venkatesan K, Liu Y, Goldfarb M. Fast-onset long-term open-state block of sodium channels by A-type FHFs mediates classical spike accommodation in hippocampal pyramidal neurons. J Neurosci 2014;34:16126–16139.
19. Wittmack EK, Rush AM, Craner MJ, Goldfarb M, Waxman SG, Dib-Hajj SD. Fibroblast growth factor homologous factor 2B: association with Nav1.6 and selective colocalization at nodes of Ranvier of dorsal root axons. J Neurosci 2004;24:6765–6775.
20. Lou JY, Laezza F, Gerber BR, et al. Fibroblast growth factor 14 is an intracellular modulator of voltage-gated sodium channels. J Physiol 2005;569:179–193.
21. Goldfarb M. Voltage-gated sodium channel-associated proteins and alternative mechanisms of inactivation and block. Cell Mol Life Sci 2012;69:1067–1076.
22. Olsen SK, Garbi M, Zampieri N, et al. Fibroblast growth factor (FGF) homologous factors share structural but not functional homology with FGFs. J Biol Chem 2003;278:34226–34236.
23. Suster ML, Kikuta H, Urasaki A, et al. Transgenesis in zebrafish with the tol2 transposon system. Methods Mol Biol 2009;561:41–63.
24. van Swieten JC, Brusse E, de Graaf BM, et al. A mutation in the fibroblast growth factor 14 gene is associated with autosomal dominant cerebellar ataxia [corrected]. Am J Hum Genet 2003;72:191–199.
25. Abu-Amero KK, Kondkar AA, Alorainy IA, et al. Xq26.3 microdeletion in a male with Wildervanck Syndrome. Ophthalmic Genet 2014;35:18–24.
26. Purunam RS, He XP, Yao L, et al. Disruption of Fgf13 causes synaptic excitatory-inhibitory imbalance and genetic epilepsy and febrile seizures plus. J Neurosci 2015;35:8866–8881.
27. Itoh N, Ornitz DM. Fibroblast growth factors: from molecular evolution to roles in development, metabolism and disease. J Biochem 2011;149:121–130.
28. Spampanato J, Kearney JA, de Haan G, et al. A novel epilepsy mutation in the sodium channel SCN1A identifies a cytoplasmic domain for beta subunit interaction. J Neurosci 2004;24:10022–10034.
29. Musa H, Kline CF, Sturm AC, et al. SCN5A variant that blocks fibroblast growth factor homologous factor regulation causes human arrhythmia. Proc Natl Acad Sci USA 2015;112:12528–12533.
30. Trudeau MM, Dalton JC, Day JW, Ranum LP, Meisler MH. Heterozygosity for a truncation mutation of the sodium channel SCN8A in a patient with cerebellar atrophy, ataxia, and mental retardation. J Med Genet 2006;43:527–530.
31. Larsen J, Carvill GL, Gardella E, et al. The phenotypic spectrum of *SCN8A* encephalopathy. Neurology 2015;84:480–489.